Journal of Oral Biology and Craniofacial Research 11 (2021) 386–392

Contents lists available at ScienceDirect

Journal of Oral Biology and Craniofacial Research

journal homepage: www.elsevier.com/locate/jobcr

Impact of biosynthesized silver nanoparticles cytotoxicity on dental pulp of albino rats (histological and immunohistochemical study)

Mervat M. Youssef [a], Merhan N. El-Mansy [a,*], Ola M. El-Borady [b], Enas M. Hegazy [a]

[a] Faculty of Dentistry, Suez Canal University, Kilo 4.5 Ring Road., Ismailia, Egypt
[b] Institute of Nanoscience and Nanotechnology, Kafrelsheikh University, 33516, Kafrelsheikh, Egypt

ARTICLE INFO

Keywords:
Cytotoxicity
Caspase-3
Dental pulp
Silver nanoparticles
VEGF

ABSTRACT

This study aimed to evaluate the potential cytotoxic effect of oral administration of silver nanoparticles (Ag-NPs) on adult albino rats' pulp tissue; due to the enormous uses of Ag-NPs in the medical and dental field. The Ag-NPs were synthesized via the green process using peels of pomegranate extract. The pomegranate-mediated Ag-NPs were subjected to morphological and spectral analysis through ultraviolet visible absorption spectra, transmission electron microscopy, Fourier transforms infrared, Zeta-potential measurements, and energy dispersive X-ray spectroscopy. The structural and morphological characterization techniques confirmed the proper synthesis of biosynthesized Ag-NPs with a size around 20 nm and the surface plasmon resonance peak within 400–450 nm. The oral cytotoxic effect of Ag-NPs was assessed through detecting the histological (hematoxylin & eosin, Masson's trichrome) and immunohistochemical (vascular endothelial growth factor (VEGF), Caspase-3 proteins) variations. The data was analyzed statistically through using the SPSS software. Dental pulp tissues of albino rats-treated with Ag-NPs revealed that most of the odontoblasts with marked hydropic degeneration, vacuolization of their cytoplasm, loss of organization and apoptosis. Marked vasodilatation and cognition of blood vessels were detected. There was weak to moderate positive reactivity to Masson's trichrome stain. There was statistically significant decrease in the expression of VEGF in the treated group and highly statistically significant increase in the expression of Caspase-3 in comparison with the control group.

Conclusion: Oral administration of Ag-NPs induced size and dose-dependent structural changes in the pulp tissue of adult male albino rats.

1. Introduction

Nanotechnology depends on the material engineering that led to improve its mechanical and physical properties. Silver nanoparticles (Ag-NPs) attracted a great attention due to its biotechnological applications and antimicrobial activity in various medical application [1]. Biomedical administration of Ag-NPs in dental applications has a great variation ranging from drug delivery to treatment of several types of diseases as oral cancer [2]. Due to its bactericidal and bacteriostatic properties specially on *Streptococus mutans*, it can be used to prevent enamel caries and inhibit plaque formation [3]. It also can be used in pulp capping, antiseptic solution, implantology and restorative fillings which aimed to avoid bacterial colonization over them and improving oral health [4]′[5].

The human intakes widespread of the diets containing silver was reached 70–90 μg/day [6]. Ag-NPs can be received through different modes of administration as pulmonary inhalation, physical contact, intravenous/intraperitoneal injection, and oral ingestion, but its particles can precipitate in many organs through different biological barriers [7]. The physicochemical properties of nanoparticles affect directly on its biological activity. The cytotoxic effect of nanomaterials relies on many crucial factors as size distribution, type of reducing agents, efficiency of ion release, particles' morphology, composition, and reactivity in the solution [8]. Moreover, it effects on bioavailability, cellular uptake, penetration to the cells and finally the therapeutic effect of the drug [9].

Systemic administration of Ag NPs in vivo induces inflammatory and cytotoxic effects as hepatotoxicity [10], blood brain barrier disruption [11], and pulmonary toxicity [12]. In vitro studies showed inflammation, reactive oxygen species (ROS), apoptosis induction, and cytotoxicity due to intracellular release of Ag ions through the interaction between Ag-NPs and surrounding environment as saliva or mucous which led to

* Corresponding author.
E-mail addresses: mervat_hawas@dent.suez.edu.eg (M.M. Youssef), merhan_elmansy@dent.suez.edu.eg, merhan_elmansy@dent.suez.edu.eg (M.N. El-Mansy), olachem_elborady@yahoo.com (O.M. El-Borady), enas_soliman@dent.suez.edu.eg (E.M. Hegazy).

https://doi.org/10.1016/j.jobcr.2021.04.002
Received 29 March 2021; Accepted 9 April 2021
Available online 14 April 2021

negative biological effects on the tissues [13]′[14]. Also, it influences with the cellular metabolism, membrane integrity and inhibit the differentiation of embryonic stem cell [15].

Angiogenesis is a complicated multistep process that led to formation of new capillaries from pre-existing vessels [16]. Ag-NPs induce cell injury through the activation of the nuclear factor kappa B-cell (NF-kβ) pathway in human endothelial cells [17]. Ag-NPs inhibit vascular endothelial growth factor (VEGF) which induce cell proliferation and promote apoptosis [18].

The caspase-3 protein is a member of the cysteine-aspartic acid protease family which plays an essential role in the execution-phase of cell apoptosis [19]. Caspase-3 plays a central role in the apoptosis execution by activation the cleavage of poly ADP-ribose polymerase (PARP)[20]. Ag-NPs induce mitochondria-mediated caspases-dependent apoptosis that led to significant increase in the permeability of mitochondria and the release of cytochrome *c*[21].

This study aimed to emphasize the potential cytotoxic effect of oral administration of silver nanoparticles on dental pulp of albino rats as its increasing used in dental applications through histological examination and immunohistochemical localization of VEGF and Caspase-3 proteins.

2. Material and methods

2.1. Fabrication of the green synthesized Ag-NPs

2.1.1. Preparation of pomegranate peel extract

Pomegranate fruits were handled from the local market. Peels of pomegranate were removed from the pulp, rinsed thoroughly with D.D. water, cut into small parts, and kept in the air for drying. 50 gm of the dried peels were weighted out and extracted with 500 ml of deionized water at 100 °C for 20 min. Afterthought, the solution was filtered through Whatman no.1 filter paper. The filtrate was centrifuged at 9000 r.p.m for 20 min to obtain a transparent yellow peel extract solution and was freshly used.

2.1.2. Biosynthesis of Ag-NPs

Silver nitrate (Ag–NO_3 < 99.9%) was obtained in Sigma Aldrich. 100 mL of an aqueous solution of Ag–NO3 (1 mM) was prepared. Then, 5 ml of freshly prepared extract filtrate was added to the salt solution and kept for incubation for 48 h with shaking. The solution color turned to brown color after 24 h, confirming the Ag ions' reduction into Ag-NPs. Then, Ag-NPs colloidal solution was centrifuged using centrifugation at 9000 rpm for 10 min. No, additional reagents were added while the extract acts as a reducing and stabilizing agent.

2.1.3. Characterization techniques for Ag-NPs

The pomegranate-mediated Ag-NPs were subjected to morphological and spectral analysis. The UV–Vis absorption spectra were detected via a Shimadzu UV-2450 spectrophotometer. The morphological properties including, size and shape were performed using a Transmission Electron Microscopy (TEM), JEOL microscope (model JEM-2010) operated at an accelerating voltage of 200 kV, attached with Gatan Camera (Model Erlangshen ES500). The structural information about the functional groups present was detected by the FTIR analysis, JASCO spectrometer over the range 4000 to 400 cm^{-1}, while the freeze-dried powder of both plant extract and Ag-NPs were grounded with KBr to form pallets. The NPs stability was displied using the Zeta-potential measurements using Zetasizer Nano ZS (Malvern) at 25 °C. The freeze-dried powdered elemental composition was screened by Energy Dispersive X-ray spectroscopy (EDX) on the scanning electron microscope (SEM), JEOL model JSM-IT100.

2.2. Experimental design

This study was carried out after the approval of ethical committee, Faculty of Dentistry, Suez Canal University (number:321/2012). Sample size calculation was performed using G*Power version 3.1.9.2[22]. The effect size was 1.25 using alpha (α) level of 0.05 and Beta (β) level of 0.05, i.e., power = 95%; the estimated minimum sample size (n) was a total of 20 samples, 10 samples for each group.

2.2.1. Animal grouping

Twenty adult male albino rats (n = 20) with an average body weight 200–230 g were used in this study. They were housed at animal house of the Faculty of dentistry, Suez Canal University, five rats per cage and kept in well ventilated room. The animals were fed dry rat pellet and drinking tap water *ad libitum*. A metallic curved oro-pharyngeal tube was used for oral administration of the drugs to the experimental animals. They were divided into two groups: Group I (n = 10) was considered as a negative control group and received deionized water daily for 21 days orally. Group II (n = 10) was considered as a treatment group and received 10 mg/kg of Ag-NPs solution with particle sizes ranging from 3 to 20 nm daily for 21 days orally [23].

At the end of the experiment which lasted 21 days, the animals were euthanized by cervical dislocation. The mandibles were dissected and immersed in 10% formalin for 48 h. For bone decalcification, fixed specimens were put in 10% EDTA for 5 weeks. Then, the specimens were washed with phosphate buffered saline, ethanol, xylol and embedded in paraffin blocks.

2.2.2. Histopathological analysis

Serial longitudinal sections (5μ) thickness was obtained using a microtome. They were mounted on adhesive-coated glass slides and stained with hematoxylin and eosin to assess any histological changes.

Masson' Trichrome stain was used for evaluating the density of collagen fibers and the presence of any collagen degeneration. The slides were examined and photographed by E−330 Olympus digital camera then the data was analyzed statistically.

Stained tissue sections were photographed with Leica DM 1000 light microscopy and Camera using Leica Application suite-LAS software in the Centre of Excellence of Molecular and Cellular Medicine (CEMCM), Suez Canal University.

2.2.3. Immunohistochemical (IHC) analysis

Five microns of the specimen's thickness were cut and mounted on positively charged slides. The steps of IHC were followed according to the instructions of manufacturer. A streptavidin-biotin complex was used for detection of VEGF and Caspase-3 proteins using mono-colonal antibodies cat No. GTX102643 and GTX30246, respectively. The optical density of the immunohistochemical staining results was assessed quantitatively through using image analyzer computer system (Image J Fuji). The area of the screen was measured by digitizing the slides under 400X objective magnification. Any nuclear and cytoplasmic staining for VEGF and Caspase-3 proteins regardless the intensity of staining was considered immune positive. All data was analyzed statistically.

2.2.4. Statistical analysis

All data were calculated, tabulated, and statistically analyzed using suitable statistical tests. A normality test was done to check normal distribution of the sample. Statistical analysis was performed using the computer program SPSS software for windows version 24.0 (Statistical Package for Social Science, Armonk, NY: IBM Corp) at significant levels 0.05 (*P*- Value ≤ 0.5).

A) Descriptive data were calculated in the form of Mean ± Standard deviation (SD).
B) Independent Student's T-test was performed for comparison of the mean differences between the two groups for each measurement.

3. Results

3.1. The structural and morphological characterization of green synthesized Ag-NPs

3.1.1. High resolution - transmission electron microscope (HR-TEM) analysis

The HR-TEM technique was employed to visualize the shape and size Ag-NPs. The TEM images demonstrated the formation of spherical NPs with an average size of 20 nm (Fig. 1, a). The selected area electron diffraction pattern (SAED) (Fig. 1, b) suggested that the synthesized Ag-NPs are crystalline in nature.

3.1.2. The energy dispersive X-Ray (EDX) analysis

Several signals corresponding to the absorption peak metallic Ag nanocrystal in the silver region (3 keV). Other peaks, identified as carbon, sodium, and copper which originated from residual extract biomolecules that serve as capping agents for the Ag-NPs (Fig. 1, c).

3.1.3. The zeta potential analysis

The surface charge and colloidal stability of the synthesized Ag-NPs were performed by measuring the zeta potential. As seen from (Fig. 1, d), The zeta potential of Ag-NPs was −17 mV, which provided sufficiently high electrostatic stabilization and preventing the NPs from agglomeration behavior.

3.1.4. The ultra-violet visible (UV–Vis) spectral analysis

When the Ag salt reacted mixed with extract, the reaction mixture's color turned from pale yellow to dark brown, indicating biosynthesis of Ag-NPs by reducing Ag^{+}. The UV–Vis absorption spectra of the extract and the prepared Ag-NPs was presented in (Fig. 1, e). The extract showed an absorption peak at 371 nm. On the other hand, the Surface Plasmon

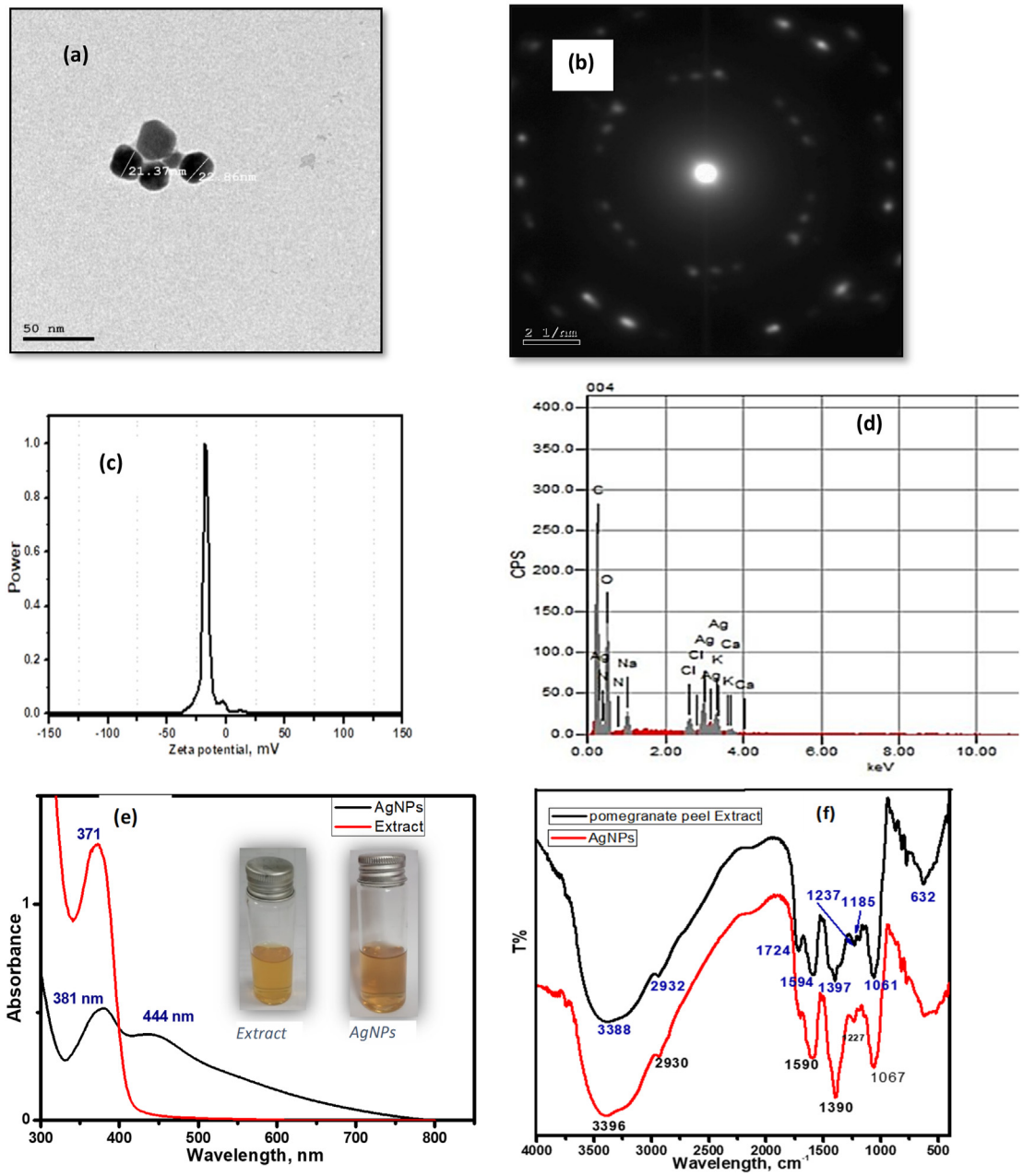

Fig. 1. Photographs showing the structural and morphological characterization of biosynthesized Ag-NPs. **(a)** The TEM image of biosynthesized Ag-NPs. **(b)** Its SAED pattern. **(c)** EDX pattern of Ag-NPs. **(d)** zeta potential of Ag-NPs. **(e)** UV–Vis absorption spectra between the extract and Ag-NPs. Note: the color changing. **(f)** FTIR spectra for the rice husk extract and Ag-NPs.

Resonance (SPR) peak characteristic for Ag-NPs was appeared at a 444 nm. The figure insert showed the color of free extract (pale yellow) and extract mediated Ag-NPs (dark brown).

3.1.5. Fourier transforms infrared (FTIR) analysis

FTIR spectroscopy was used to identify the functional group and biomolecules available in the plant extract, which is a reducer and stabilizer. The FTIR spectra for both the extract and Ag-NPs, were presented in (Fig. 1, f). The peak at 3388 cm−1 assigned to the hydroxyl group present in flavonoid and phenolic or amine; this band appeared for Ag-NPs at 3396 cm^{-1}, the shift occurred indicative of the chelating between extract and NPs via OH group. The C–H stretching of alkane was observed at 2932 and 2930 cm^{-1} for extract and Ag-NPs, respectively. While the C═O stretching peak of the amide group in protein was seen at 1724 cm^{-1} in the extract but its corresponding vibration peak in the Ag-NPs is almost disappeared, as evidence of the attachment of the Ag-NPs to the extract by this group. Furthermore, the aromatic amine and the C–N stretching vibration peak were observed around 1390 cm^{-1} and 1060 cm^{-1}, respectively for both extract and Ag-NPs. As summarized from FTIR studies, Ag-NPs suggested to being bonded to extract components through the OH and C═O present in the extract component.

3.2. Histopathological evaluation

Group I (Negative control): The pulp tissue of the negative control specimens was formed of loose vascular connective tissue bound with a layer of odontoblasts which arranged at the periphery of the pulp core and had processes extending to dentin. The pulp core consisted of the fibroblasts and collagen fibres that were embedded in an amorphous ground substance. Inflammatory cells were scattered through the pulp. The pulp had vascular and neural elements (Fig. 2 A, B). The collagen fibres of the pulp revealed normal distribution with strongly positive staining reactivity to Masson's trichrome stain (Fig. 2, G).

Group II (Ag-NPs-treated group): Examination of the pulp tissue that was taken from the rats treated with Ag-NPs solution for 21 days revealed marked degeneration, and apoptosis in the odontoblastic layer. Moreover, most of the odontoblasts showed atrophy, hydropic and/or fatty degeneration, vacuolization of their cytoplasm, loss of organization and their separation from the dentin. Fibroblasts revealed varying degree of necrosis manifested as cytoplasmic edema with hydropic or fatty degeneration. A lot of vascular changes in the form of marked vasodilatation, dilacerations, stagnation, cognition of blood and occlusion the vascular channels (partial and/or complete) were detected. Some cases showed extravasation of RBCs and infiltration of inflammatory cell

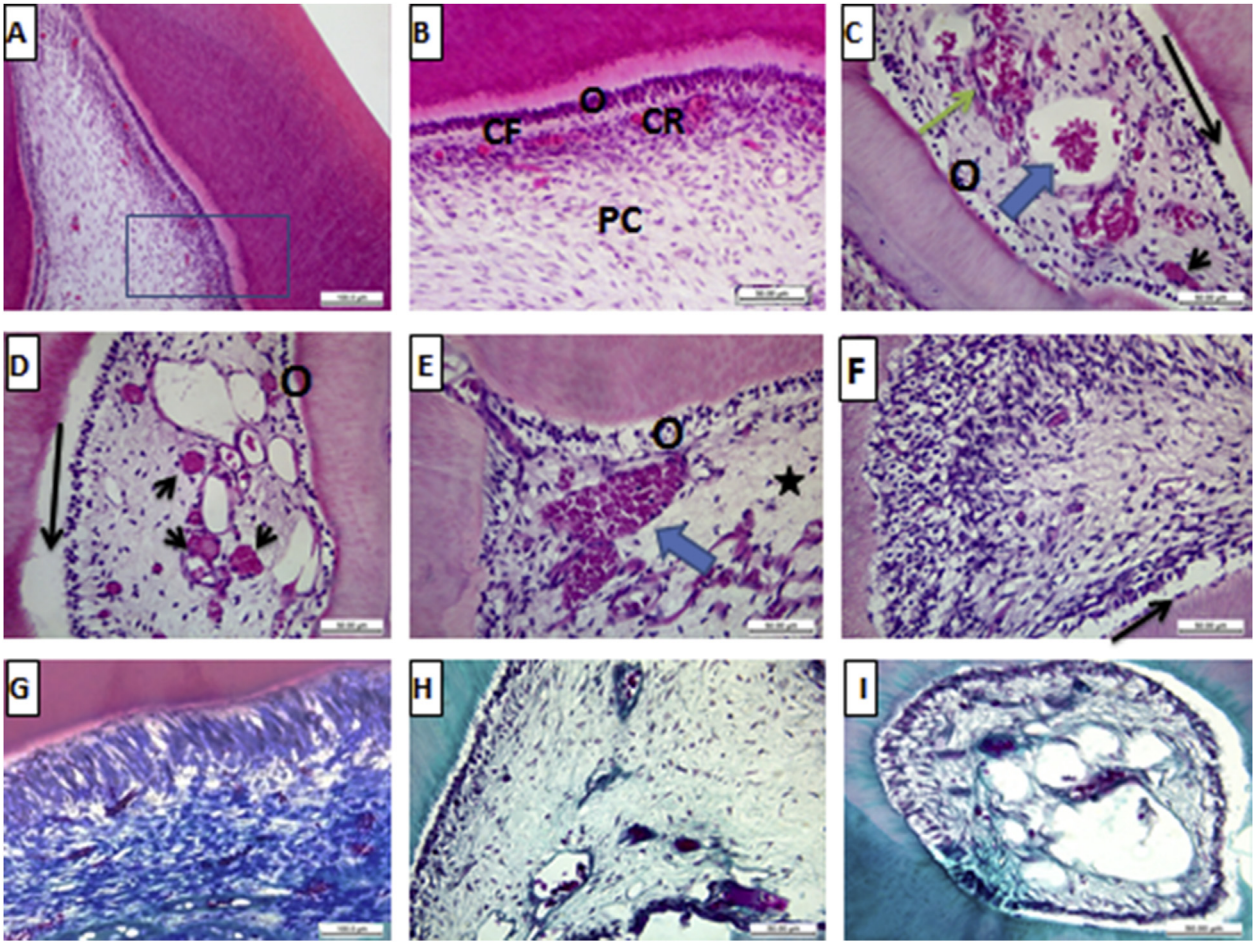

Fig. 2. Histological photomicrographs showing the pulp tissue stained with H& E stain **(A: F)** and Masson trichrome stain **(G: I)**. **A, B)** showing the pulp of the control group with normal histological structure; odontoblastic layer **O**, cell-free zone **CF**, cell-rich zone **CR** and central pulp core **PC** (X 100 & 400). **C: E)** showing the pulp of Ag-NPs-treated group with odontoblastic atrophy and degeneration **O**, separation of the odontoblastic layer from dentin **black arrow**, tissue degeneration in the pulp core **star**, congestion of blood vessels with RBCs **blue arrow**, extravasation of RBCs **green arrow**, and occlusion of blood vessels **black arrow heads** (X 400). **F)** showing marked hydropic/fatty degeneration in the odontoblastic and sub odontoblastic layer with massive infiltration of inflammatory cell (X 400). **G)** showing strongly positive reactivity of the collagen fibers with Masson's trichrome stain in the negative control group (X 400). **H, I)** showing weak to moderate positive reactivity to the Masson's trichrome stain in Ag-NPs-treated group (X 400).

(Fig. 2, C: F). Degeneration and dissociation of the collagen fibers were noticed that showed weak to moderate positive reactivity to the Masson's trichrome stain (Fig. 2H, I). Histomorphometric analysis of the mean total collagen density in the pulp tissue of the specimens treated with Ag-NPs showed highly statistically significant decrease (71.56 ± 9.47) in comparison to the control group which did not receive any type of treatment (27.76 ± 6.70) Table 1.

3.3. Immunohistochemical (IHC) evaluation

Immunohistochemical expression of VEGF protein is helpful to detect any new blood vessel formation. Sections of the dental pulp of the negative control group revealed moderate nuclear and cytoplasmic staining reaction to VEGF mono-colonal antibody (Fig. 3, A). While those treated with Ag-NPs solution revealed marked reduction in the staining reactivity compared to their controls (Fig. 3, B &C). There was highly statistically significant decrease in group II (12.72 ± 3.49) in comparison to group I (36.89 ± 7.53) Table 1.

Immunohistochemical expression of Caspase-3 protein is helpful to detect any apoptotic changes. The dental pulp of negative control group revealed weak nuclear and cytoplasmic staining reaction to caspase-3 mono-colonal antibody (Fig. 3, D). in comparison with the group treated with Ag-NPs solution that showed strong immune staining reaction (Fig. 3, E &F). There was highly statistically significant increase in group II (119.02 ± 15.27) in comparison to group I (32.90 ± 13.27) Table 1.

4. Discussion

In terms of the environmental concerns, green methods used for the preparation of silver nanoparticles from plant extract tended to reduce the drawbacks associated with the conventional methods. Bio-reduction of metallic ions can be easily achieved due to its ease of synthesis and higher stability. The structural and morphological characterization of the green synthesized Ag-NPs in the present study were online with various studies [24]′[25].

Although silver nanoparticles have many medical and dental application due to their bacteriostatic and bactericidal effects. They have potential risks to human health. Ferdous and Nemmar, (2020)[26] reported many previous in vitro and in vivo studies focused on Ag-NPs-induced toxicity to various organs. The present study used the albino rats which received 10 mg/kg Ag-NPs solution with particle sizes about 20 nm per day for 21 consecutive days to evaluate the potential cytotoxic effect on the pulp tissue. Their particle sizes might passively penetrate cell membranes coincided with that presented by with Shahare et al. (2013)[23] who demonstrated that this dose was the best dose to induce prominent cytotoxic effects on small intestine mucosa of mice. Together with Van Der Zande and coworkers, (2012)[27] who studied the cytotoxic effect of oral administration of Ag-NPs (15–20 nm) in rats for 28 days. This study observed that the nano preparation itself and the silver ion released from the preparation play a synergistic effect on inducing the cytotoxicity. On the other hand, De Jong et al. (2013)[28] observed that oral administration of Ag-NPs (22 nm) did not show severe systemic toxicity due to low absorption of the lung and gastrointestinal tract (GI-tract) in comparison with intravenous administration. Our experiment was consistent with previous study done by Hernández--Sierra et al. (2008)[3]studied the cytotoxic effect of Ag-NPs on the fibroblastic cells of the periodontal tissue which depend mainly on the particle size. Less than 20 nm showed significant increase in the cytotoxicity on the contrary to 80–100 nm in diameter which reveal increase in the cell viability.

Systemic administration of Ag-NPs leads to translocation of these particles to different body parts and induces cytotoxic effects through ROS release, release of Ag ions, mitochondrial membrane damage and apoptosis induction [13]′[14]. Yamazaki et al. (2006)[29] were online with the previous hypothesis who reported that Ag ions are the main cause of mitochondrial damage and their cytotoxicity through abrogation of N acetyl cysteine (NAC). In contrary to this study, Eom and Choi, (2010)[14] reported that only thiol containing compounds (NAC), methionine and cysteine, played a significant role in prevention of Ag-NPs cytotoxicity through neutralizing the effect of Ag ions. So, the authors hypothesized that free radicals do not play a prominent role in eliminating the cytotoxicity.

The histological findings in the group-treated with Ag-NPs of the present study showed significant epithelial and collagen degeneration, congested blood vessels with RBCs and increase in the inflammatory cells. Comparable histological changes were recorded by Sarhan and Hussein, (2014)[30] who found that after intraperitoneal administration of Ag-NPs, there were significant hydropic changes within the epithelium, cytoplasmic vacuolations with edematous mitochondria and aggregation of fat globules. Moreover, Mazen et al., (2017)[31] confirmed that after intraperitoneal administration of Ag-NPs, there was structural alterations in the form of depletion of lymphocytes, degeneration, and apoptosis (increase in the optical density of caspase 3). On contrary to our study, Nadworny et al., (2010)[32] confirmed that there was significant decrease in the number of inflammatory cells due to apoptosis after the treatment with Ag-NPs and decreased the pro-inflammatory cytokines as prostaglandins, interleukin-1 (IL-1), tumor necrosis factor (TNF) fibroblast growth factor (FGF) and tumor growth factor (TGF).

In the current study, there was a highly significant increase in the expression of Caspase-3 in the group-treated with Ag-NPs in comparison with the negative control group. Mammucari and Rizzuto, (2010)[33] reported that the early stage in apoptosis is dissipation of mitochondrial membrane potential (MMP). Ag-NPs-treated cell line showed significant dissipation of MMP and increase in the number of apoptotic cells when compared to control. Online with our results, AshaRani et al., (2009)[34] who revealed that Ag-NPs influences the cell viability and apoptotic process through mitochondrial damage due to the destructive effect of oxidative stresses that end with DNA damage. Gurunathan et al., (2009)[35] confirmed that Ag-NPs-mediated apoptosis related with down-regulation of Bcl-2 and activation of proapoptotic proteins, p53 and caspase-3 signaling.

One of the interesting findings in this study was the multiple vascular changes which were observed in the group-treated with Ag-NPs in comparison with the negative control group. These changes included marked vasodilatation, dilacerations, stagnation, cognition of blood and occlusion the vascular channels as well as significant decrease in the expression of VEGF. Online with our results, Gurunathan et al., (2009)[35] considered that Ag-NPs is an antiangiogenic agent through eliminating the expression of VEGF via inhibition of HIF-1α protein (oxygen-sensitive transcription factors) accumulation that led to deactivation of VEGF transcription. Moreover, it contributes to the inhibition of new blood micro vessels formation due to inactivation of PI3K/Akt which regulate the growth factors and the transcriptional factors. The basal expression of VEGF after Ag-NPs application to cell lines was dose-dependent manner [36].

Table 1
Image J analysis.

Markers	Groups	Mean ± St. Deviation	Independent-t-test	Sig.
Caspase	1	32.90 ± 13.27	−9.517	0.000**
	2	119.02 ± 15.27		
VEGF	1	36.89 ± 7.53	6.509	0.000**
	2	12.72 ± 3.49		
Masson Trichrome	1	71.56 ± 9.47	8.442	0.000**
	2	27.76 ± 6.70		

**; means significant differences between groups using Independent-t-test at $P < 0.05$.

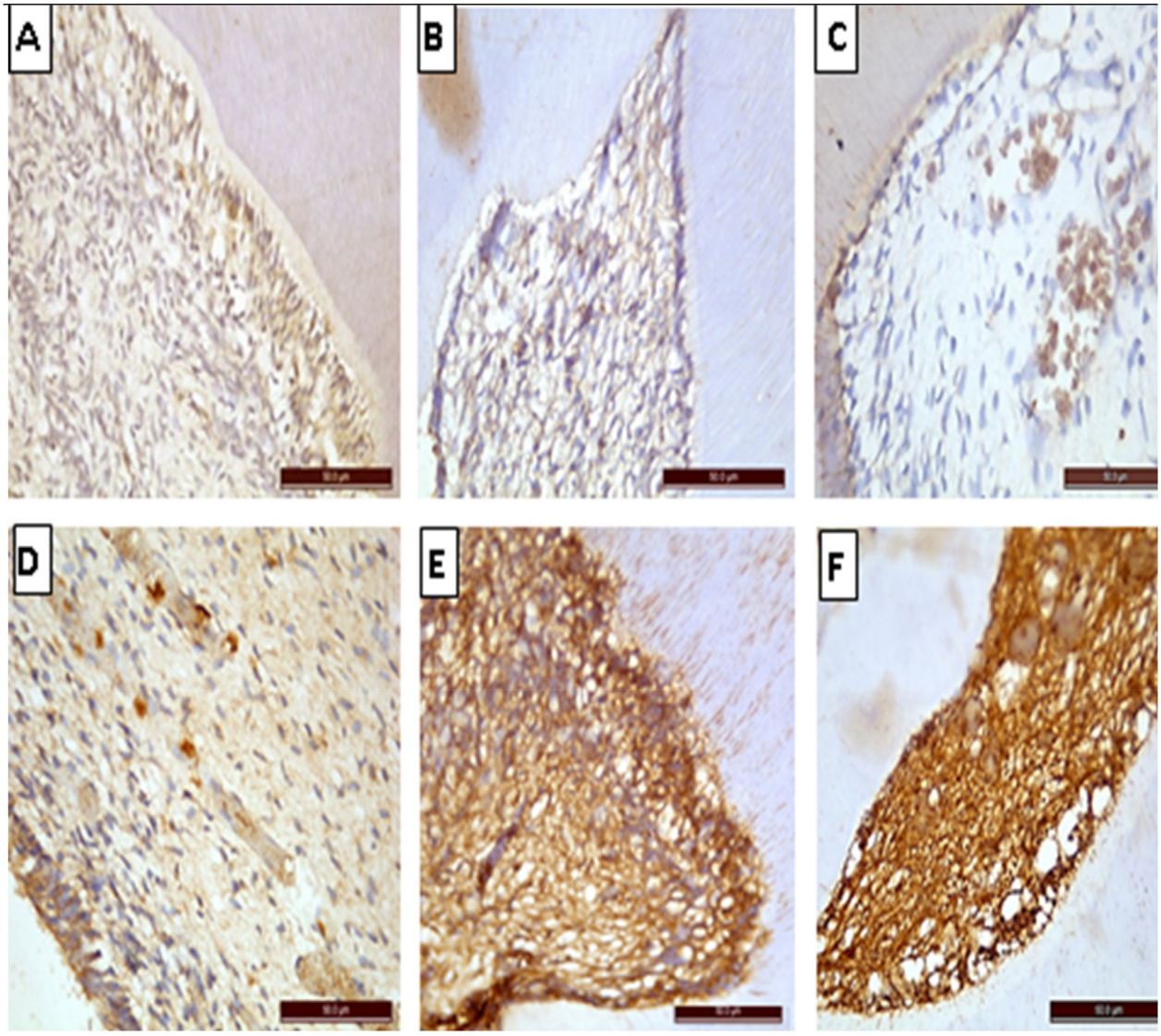

Fig. 3. Photomicrographs of immunohistochemical-stained sections of the pulp tissue of different groups (X400). **A)** Control group showing moderately positive staining reactivity to VEGF mono-colonal antibody. **B, C)** Treatment group showing marked reduction in the staining reactivity to VEGF. **D)** Control group showing weak positive staining reaction to caspase 3 mono-colonal antibody. **E, F)** Treatment group showing strong positive staining reaction of pulp cells, fibers & blood vessels to caspase 3.

5. Conclusion

Oral administration of Ag-NPs that commonly used in various dental application induced size and dose-dependent structural changes in the pulp tissue of adult male albino rats. We recommended that the future clinical studies should be give great attention to the size of Ag-NPs when incorporated into the restorative materials as in operative or endodontic treatment to avoid its possible toxic effect on the pulp tissue.

Ethical statement

This study was carried out after the approval of Research Ethics' committee, Faculty of Dentistry, Suez Canal University (number: 321/2021) under the guidelines of "WHO-2011" standards.

Funding

This research did not receive any specific grant from funding agencies.

Declaration of competing interest

The authors declared that they had no competing financial interests or personal relationships that might affect this research.

References

1. Gravante G, Caruso R, Sorge R, Nicoli F, Gentile P, Cervelli V. Nanocrystalline silver: a systematic review of randomized trials conducted on burned patients and an evidence-based assessment of potential advantages over older silver formulations. *Ann Plast Surg*. 2009;63:201–205. https://doi.org/10.1097/sap.0b013e3181893825.
2. Hamouda IM. Current perspectives of nanoparticles in medical and dental biomaterials. *J Biomed Res*. 2012;26:143–151. https://doi.org/10.7555/jbr.26.20120027.
3. Hernández-Sierra JF, Ruiz F, Pena DC, et al. The antimicrobial sensitivity of Streptococcus mutans to nanoparticles of silver, zinc oxide, and gold. *Nanomedicine*. 2008;4:237–240. https://doi.org/10.1016/j.nano.2008.04.005.
4. Zhao L, Wang H, Huo K, et al. Antibacterial nano-structured titania coating incorporated with silver nanoparticles. *Biomaterials*. 2011;32:5706–5716. https://doi.org/10.1016/j.biomaterials.2011.04.040.
5. Cheng L, Weir MD, Xu HH, et al. Effect of amorphous calcium phosphate and silver nanocomposites on dental plaque microcosm biofilms. *J Biomed Mater Res B Appl Biomater*. 2012;100:1378–1386. https://doi.org/10.1002/jbm.b.32709.

6. Wijnhoven SW, Peijnenburg WJ, Herberts CA, et al. Nano-silver–a review of available data and knowledge gaps in human and environmental risk assessment. *Nanotoxicology*. 2009;3:109–138. https://doi.org/10.1080/17435390902725914.
7. Wang Z, Qu G, Su L, et al. Evaluation of the biological fate and the transport through biological barriers of nanosilver in mice. *Curr Pharmaceut Des*. 2013;19:6691–6697. https://doi.org/10.2174/1381612811319370012.
8. Carlson C, Hussain SM, Schrand AM, et al. Unique cellular interaction of silver nanoparticles: size-dependent generation of reactive oxygen species. *J Phys Chem B*. 2008;112:13608–13619. https://doi.org/10.1021/jp712087m.
9. Albanese A, Tang PS, Chan WC. The effect of nanoparticle size, shape, and surface chemistry on biological systems. *Annu Rev Biomed Eng*. 2012;14:1–6. https://doi.org/10.1146/annurev-bioeng-071811-150124.
10. Tiwari DK, Jin T, Behari J. Dose-dependent in-vivo toxicity assessment of silver nanoparticle in Wistar rats. *Toxicol Mech Methods*. 2011;21:13–24. https://doi.org/10.3109/15376516.2010.529184.
11. Yang Z, Liu ZW, Allaker RP, et al. A review of nanoparticle functionality and toxicity on the central nervous system. *J R Soc Interface*. 2010;7:411–422. https://doi.org/10.1098/rsif.2010.0158.focus.
12. Sung JH, Ji JH, Yoon JU, et al. Lung function changes in Sprague-Dawley rats after prolonged inhalation exposure to silver nanoparticles. *Inhal Toxicol*. 2008;20:567–574. https://doi.org/10.1080/08958370701874671.
13. George S, Lin S, Ji Z, et al. Surface defects on plate-shaped silver nanoparticles contribute to its hazard potential in a fish gill cell line and zebrafish embryos. *ACS Nano*. 2012;6:3745–3759. https://doi.org/10.1021/nn204671v.
14. Eom HJ, Choi J. p38 MAPK activation, DNA damage, cell cycle arrest and apoptosis as mechanisms of toxicity of silver nanoparticles in Jurkat T cells. *Environ Sci Technol*. 2010;44:8337–8342. https://doi.org/10.1021/es1020668.
15. Park MV, Neigh AM, Vermeulen JP, et al. The effect of particle size on the cytotoxicity, inflammation, developmental toxicity, and genotoxicity of silver nanoparticles. *Biomaterials*. 2011;32:9810–9817. https://doi.org/10.1016/j.biomaterials.2011.08.085.
16. Carmeliet P. Angiogenesis in life, disease, and medicine. *Nature*. 2005;438:932–936. https://doi.org/10.1038/nature04478.
17. Shi J, Sun X, Lin Y, et al. Endothelial cell injury and dysfunction induced by silver nanoparticles through oxidative stress via IKK/NF-κB pathways. *Biomaterials*. 2014;35:6657–6666. https://doi.org/10.1016/j.biomaterials.2014.04.093.
18. Kalishwaralal K, Banumathi E, Pandian SR, et al. Silver nanoparticles inhibit VEGF induced cell proliferation and migration in bovine retinal endothelial cells. *Colloids Surf B Biointerfaces*. 2009;73:51–57. https://doi.org/10.1016/j.colsurfb.2009.04.025.
19. Alnemri ES, Livingston DJ, Nicholson DW, et al. Human ICE/CED-3 protease nomenclature. *Cell*. 1996;87:171. https://doi.org/10.1016/s0092-8674(00)81334-3.
20. Le Rhun Y, Kirkland JB, Shah GM. Cellular responses to DNA damage in the absence of poly (ADP-ribose) polymerase. *Biochem Biophys Res Commun*. 1998;245:1–10. https://doi.org/10.1006/bbrc.1998.8257.
21. George BP, Kumar N, Abrahamse H, Ray SS. Apoptotic efficacy of multifaceted biosynthesized silver nanoparticles on human adenocarcinoma cells. *Sci Rep*. 2018;8:1–4. https://doi.org/10.1038/s41598-018-32480-5.
22. Faul F, Erdfelder E, Lang AG, Buchner AG. * Power 3: a flexible statistical power analysis program for the social, behavioral, and biomedical sciences. *Behav Res Methods*. 2007;39:175–191. https://doi.org/10.3758/bf03193146.
23. Shahare B, Yashpal M, Gajendra A. Toxic effects of repeated oral exposure of silver nanoparticles on small intestine mucosa of mice. *Toxicol Mech Methods*. 2013;23:161–167. https://doi.org/10.3109/15376516.2013.764950.
24. El-Borady OM, Ayat MS, Shabrawy MA, Millet P. Green synthesis of gold nanoparticles using Parsley leaves extract and their applications as an alternative catalytic, antioxidant, anticancer, and antibacterial agents. *Adv Powder Technol*. 2020;31:4390–4400. https://doi.org/10.1016/j.apt.2020.09.017.
25. Nishanthi R, Malathi S, Palani P. Green synthesis and characterization of bioinspired silver, gold and platinum nanoparticles and evaluation of their synergistic antibacterial activity after combining with different classes of antibiotics. *Mater Sci Eng*. 2019;96:693–707. https://doi.org/10.1016/j.msec.2018.11.050.
26. Ferdous Z, Nemmar A. Health impact of silver nanoparticles: a review of the biodistribution and toxicity following various routes of exposure. *Int J Mol Sci*. 2020;21:2375. https://doi.org/10.3390/ijms21072375.
27. Van Der Zande M, Vandebriel RJ, Van Doren E, et al. Distribution, elimination, and toxicity of silver nanoparticles and silver ions in rats after 28-day oral exposure. *ACS Nano*. 2012;6:7427–7442. https://doi.org/10.1021/nn302649p.
28. De Jong WH, Van Der Ven LT, Sleijffers A, et al. Systemic and immunotoxicity of silver nanoparticles in an intravenous 28-day repeated dose toxicity study in rats. *Biomaterials*. 2013;34:8333–8343. https://doi.org/10.1016/j.biomaterials.2013.06.048.
29. Yamazaki T, Yamazaki A, Hibino Y, et al. Biological impact of contact with metals on cells. In: *Vivo 20: 605–611*. 2006. PMID: 17091767.
30. Sarhan OM, Hussein RM. Effects of intraperitoneally injected silver nanoparticles on histological structures and blood parameters in the albino rat. *Int J Nanomed*. 2014;9:1505–1517. https://doi.org/10.2147/ijn.s56729.
31. Mazen N, Saleh E, Mahmoud A, Shaalan A. Histological and immunohistochemical study on the potential toxicity of sliver nanoparticles on the structure of the spleen in adult male albino rats. *Egy J Histol*. 2017;40:374–387. https://doi.org/10.21608/EJH.2017.4662.
32. Nadworny PL, Landry BK, Wang J, Tredget EE, Burrell RE. Does nanocrystalline silver have a transferable effect? *Wound Repair Regen*. 2010;18:254–265. https://doi.org/10.1111/j.1524-475x.2010.00579.x.
33. Mammucari C, Rizzuto R. Signaling pathways in mitochondrial dysfunction and aging. *Mech Ageing Dev*. 2010;131:536–543. https://doi.org/10.1016/j.mad.2010.07.003.
34. AshaRani PV, Mun GLK, Hande MP, Valiyaveettil S. Cytotoxicity and genotoxicity of silver nanoparticles in human cells. *ACS Nano*. 2009;3:279–290. https://doi.org/10.1021/nn800596w.
35. Gurunathan S, Lee KJ, Kalishwaralal K, Sheikpranbabu S, Vaidyanathan R, Eom SH. Antiangiogenic properties of silver nanoparticles. *Biomaterials*. 2009;30:6341–6350. https://doi.org/10.1016/j.biomaterials.2009.08.008.
36. Lee KS, Kim SR, Park SJ, et al. Mast cells can mediate vascular permeability through regulation of the PI3K-HIF-1 alpha-VEGF axis. *Am J Respir Crit Care Med*. 2008;178:787–797. https://doi.org/10.1164/rccm.200801-008oc.